

# End of Project Report on Proof of Concept Research on Smart X-ray Optics

Principal Investigator: Dr Peter Doel, UCL

Co-Investigators: Prof Alan Michette (KCL), Prof Alan Smith (MSSL), Prof Melvyn Folkard (Grays Cancer Institute), Dr Tom Stevenson (UoE)

## 1. Introduction

Results are presented of a one year proof of concept research programme into Smart X-ray Optics. The ultimate aim is to develop new X-ray optical systems particularly applying the techniques of active/adaptive optics. Applications of such technology range from medical imaging to astronomy. The proof of concept research programme's goals were to investigate key technological issues and identify the most effective ways forward.

At X-ray wavelengths shorter than  $\sim 1\text{nm}$  focusing is only possible either by grazing incidence reflection or by the use of zone plates. While zone plates can provide high performance they are limited both by their size (typically  $<0.5\text{mm}$  in diameter) and their energy and bandpass (the focal length of a zone plate is strongly wavelength dependent ( $\sim 1/\lambda$ ) and so refocusing is needed whenever the wavelength is changed). Below  $0.1\text{nm}$  zone plates pose problems since the zones have to be thick (for efficiency) and outer zone widths have to be wide so that aspect ratios are reasonable, typically limiting spatial resolutions to a few microns. It is important to note that zone plates cannot be adaptive.

Not only have adaptive techniques the potential to delivery very high resolution systems (focal spots below  $<1\ \mu\text{m}$ , imaging resolutions  $\ll 1$  arc second) they also permit scanning or image optimisation in different parts of the field of view. The quality of the image across a traditionally focused X-ray image plane is inevitably a compromise and it would be a major advance to be able to locally improve the image quality around an object of interest during a targeted investigation, (e.g., for medical imaging or astronomy).

## 2 Active Conic Section large thin shell mirrors

Large scale X-ray optics are used in satellite borne astronomical observatories such as XMM-Newton. To get high efficiency many thin grazing incident mirrors need to be nested together, however due to the shells thinness and the method of manufacture form errors occur which severely limits the resolution attainable. If such mirrors could be actively controlled then considerable science gains would be achieved. The research undertaken was to investigate the key technologies to enable thin active mirrors and to develop modelling capabilities to design a full system.

### 2.1 Computer modelling

To test the possible methods required to actuate a thin x-ray type mirror a computer model base was devised using FEMLAB – a multi-physics, finite element analysis suite of software. This allowed us to create full piezo-electric-mechanical models and also provided an easy interface with MATLAB for extra analysis or optimisation of parameters where necessary.

Initial experiments were to see how accurate a given parabolic shape could be obtained starting from a flat mirror strip. Based on available piezo-ceramic plate sizes from PI ceramics, the dimensions of the piezo plate was set to  $70 \times 25 \times 0.5\text{mm}$  with a number of electrodes sub-divided along its length. The mirror substrate bonded to the piezo-plate was dimensioned at  $75 \times 25 \times 1\text{mm}$  as provided by Crystran Ltd.

The entire FEMLAB model (see Figure 1) was exported to a MATLAB m-file and incorporated into an optimisation loop using the Optimisation Toolbox. Good initial voltages for the electrodes were determined by hand. The best RMS fit to the parabola obtained during these optimisations for a 10-electrode model was  $0.16\ \mu\text{m}$ . Increasing the electrode density to 15 improves the RMS to  $0.11\ \mu\text{m}$ , and a 20-electrode pattern obtains an RMS of  $0.09\ \mu\text{m}$ . It is possible that the RMS fit could be improved from these figures if longer optimisations are allowed or different routines devised. The parameter space for the 20-electrode model is very large and there has been insufficient computing time to explore it to a satisfactory extent.

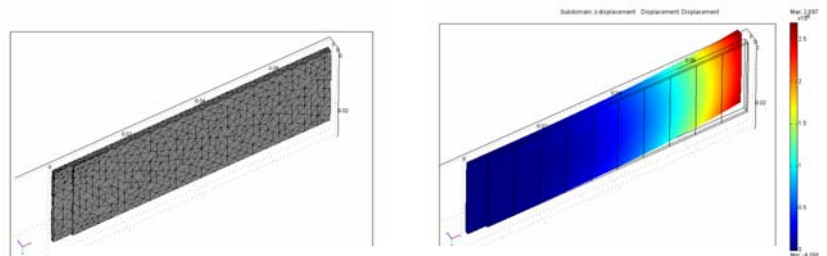


Figure 1: Showing various modelling stages in FEMLAB for the 10-electrode mirror strip.

### 2.2 Laboratory verification of the FEMLAB models

To provide verification of the FEMLAB model base, common systems were constructed in FEMLAB and then assembled and tested in the laboratory. This research also investigated the influence functions from segmented piezo-devices – a key part of an active mirror system. The measurements were taken using a WYKO 6000 interferometer ( $\lambda=613\text{nm}$ ), where possible surface maps were taken but in some cases surface deformations exceeded the range of the interferometer and so just the fringe intensity pattern was recorded.

The piezo-ceramic used in the experiments was obtained from PI Ceramics and was their PIC255 formulation, offering a suitable balance of material properties and mid-range charge constants ( $d_{31}$ ,  $d_{33}$ ).

Initial constructions were based on the model shown in Figure 2(a). Plates of piezo-ceramic (70x25x0.5mm) were bonded to flat mirrored glass plates (75x25x1mm) of approximately  $\lambda/2$  across the entire surface with a silver conductive epoxy (CHO-BOND 584-29). Unfortunately the effects of glue shrinkage caused the thin composite to warp by such an amount as to make a significant proportion of the mirror surfaces beyond the measurement range of the interferometer. Comparisons with the computer model in these cases were therefore not reliable

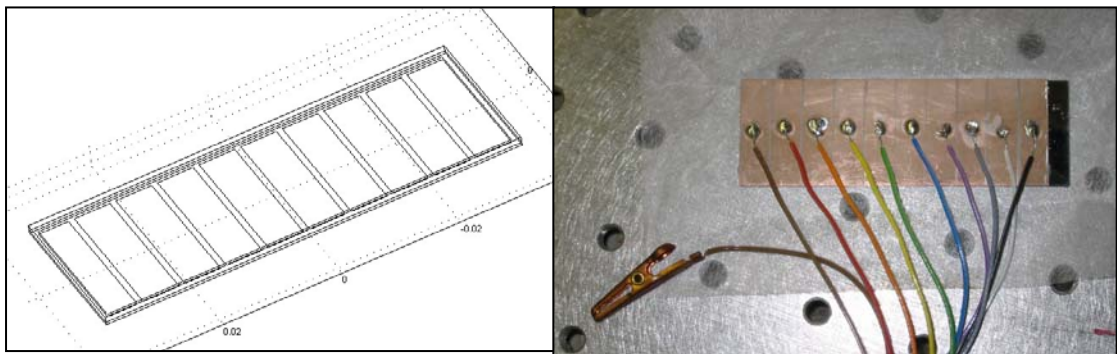


**Figure 2:** 10-electrode etched piezo plate bonded to 1mm thick flat rectangular mirror. For scale the spacing of holes on the optical table is 25mm.

A thicker glass substrate (75mm diameter, 4mm thick) was polished at UCL to a figure flatness of  $<200\text{nm}$  over the surface. An in-house conductive glue formulation was devised using  $10\mu\text{m}$  silver flake and epoxy. On bonding the hexagonal piezo-ceramic plates to the back of this mirror, warping of the mirror due to shrinkage was approximately radially symmetric and only altered the surface flatness to  $<300\text{nm}$  figure error, so remained within the measurable range of the interferometer. Figure 3(b) shows the completed structure with the FEMLAB model to the left. Differences between the structures exist due to computing memory restrictions which limited the number of elements in the FEA, so no gaps between the segments could be incorporated. It is likely that this difference is the reason why simulated values of actuator displacement are lower than those in the lab – no gaps would result in a stiffer overall structure and the influence functions of the individual segments are more closely inter-linked.

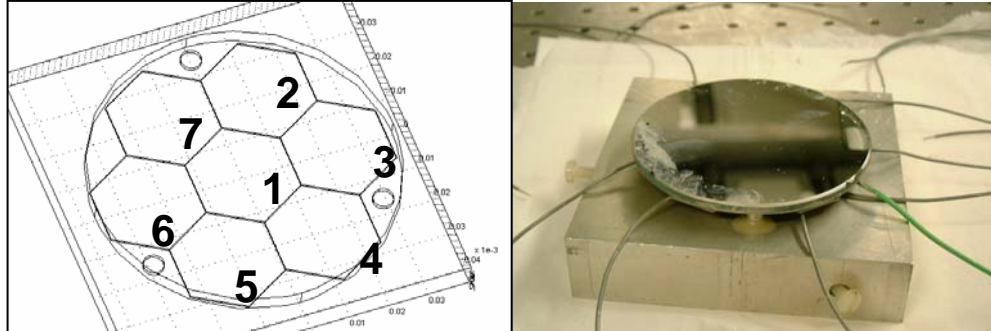


**Figure 3:** Circular mirror with 7 hexagonal piezo-ceramic pieces bonded on one side. (a) FEMLAB model of mirror, electrodes are numbered for reference; (b) similar mirror constructed in laboratory.

The plot in Figure 4 shows the results of applying a set of voltages to each of the different actuators in turn. As a representation of the different types of actuator measurements were taken for the central electrode (actuator 1) and an edge-side electrode (actuator 2). The difference between modelled and measured displacements for actuator 1 varies from 80% to 74% (low to high voltage), whilst for actuator 2 the difference starts at 98% and drops to 84% at higher voltages. The larger discrepancy for the central actuator is expected given the previous discussion on no-gaps between actuators in the computer model – edge electrodes have a free, non-constrained edge, unlike the central electrode in simulations.

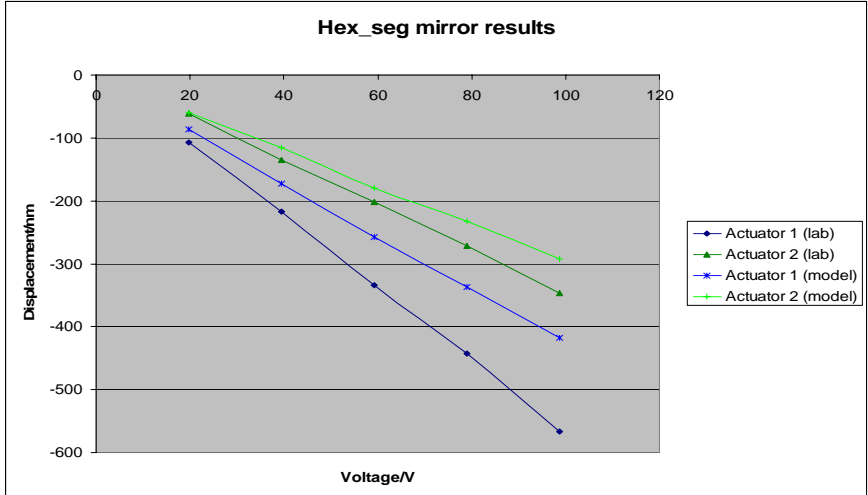


**Figure 4:** Graph showing displacement measured at centre electrode (actuator 1) and an edge electrode (actuator 2) for computer model and lab structure.

Additional experiments were performed to show the effect of applying patterns of voltage across the various actuators. Figure 5 shows a set of these as modelled in FEMLAB and then measured in the laboratory. The observed patterns agree to a reasonable

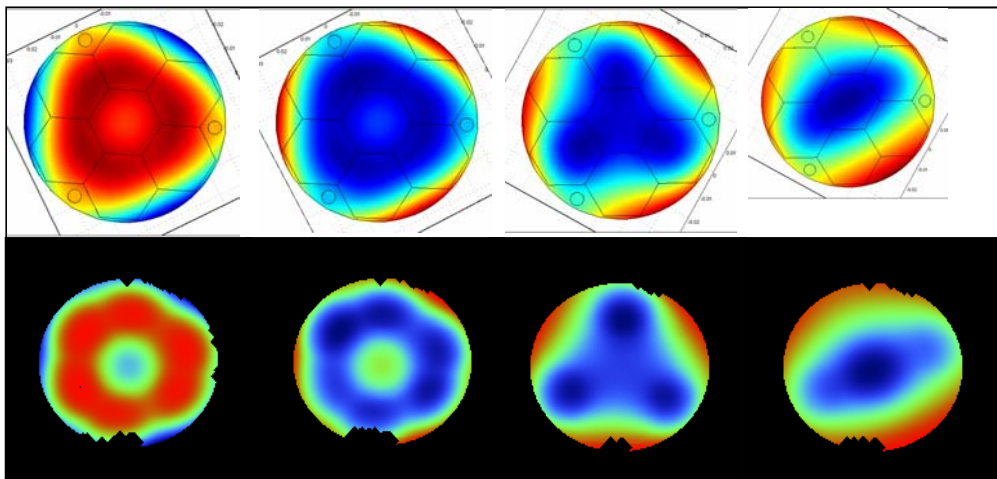


**Figure 5:** Various voltage patterns applied to the segmented hexagonal mirror in the model (top) and the corresponding lab measurement directly below (a-d left to right).

extent and measured displacements also agree within 25%. In some cases (Figure 5(d)) the comparison is very close - the central displacement as measured in the lab is 315nm and 305nm in the model.

### 2.3. Testing on the XMM-Newton mirror shell

The aim was to investigate suitable piezo-electrics capable of altering the shape of the large nickel mirror shell using only low voltages (~100V). The first test (Figure 6) was to bond a grid of 18, 5x15x0.5mm flat piezo-ceramic pieces to the outer surface of the shell. A system of mirrors and a suitable cylindrical lens were used to allow interferometric measurement of the surface – large distortions and high frequency vibration of the shell made this difficult. On bonding, the grid pattern could be seen in the fringe patterns – highlighting the importance for the future in using piezo-ceramics that can conform to the surface by nature of their flexibility or by moulding them to the exact required shape. Figure 6(a) inset top, shows the surface of the mirror with the electrode all turned off – sections of the mirror are beyond the measurement range of the interferometer; figure 6(b) shows the effect when a selection of voltages are applied to the electrodes – the mirror surface is easily deformed and has brought parts of the surface previous unmeasurable within range of the interferometer.

A promising approach that was investigated was using Macro-Fibre Composite (MFC). Samples were ordered from Smart Materials Ltd and figure 7 shows a piece of this bonded to the outer shell of the XMM mirror. Although extremely thin, this was able to deform the mirror – surface measurements were not possible for this so a set of fringe intensity patterns are provided to illustrate the change.

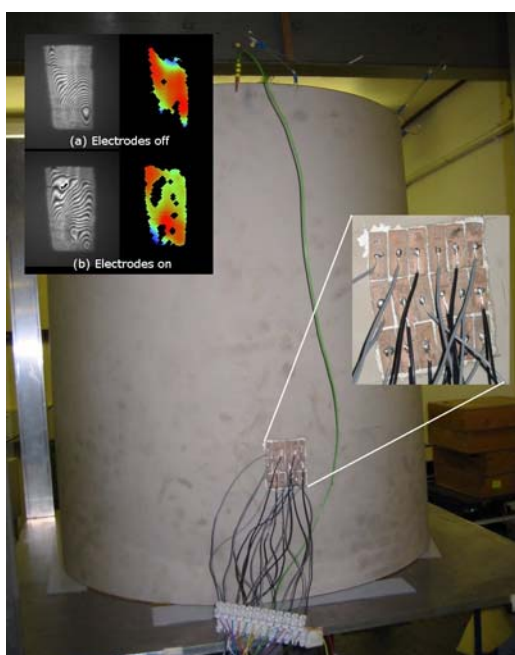


**Figure 6:** The spare XMM mirror shell mounted on a custom table at OSL. The grid of piezo plates is shown, conductively glued to the outer side. The upper inset pictures are interferometer measurements of the inner surface showing the difference with and without basic actuation.

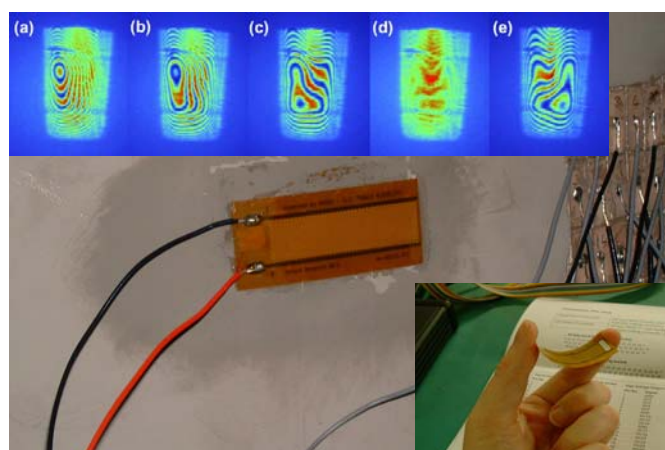


**Figure 7:** A 40x10mm piece of Macro-Fibre Composite bonded to the outside of the XMM shell. Inset top, shows the fringe intensity patterns as measured with the WKYO interferometer when voltages of (a) -170; (b) -95; (c) 0; (d) 95 and (e) 170 are applied. Inset bottom, shows the composite before bonding, demonstrating how thin, flexible and robust the material is.

The research has shown that thin piezo-ceramics can be successfully bonded and used to activate a thin X-ray shell. Segmented unimorph designs have also been tested – a key aspect of a future design. Future areas of work will include shaped large piezo ceramic unimorphs and low surface deformation bonding techniques.

### 3. Microstructured Optical Arrays (KCL, SMC, GCI)

The aim was to improve the performances of capillary-type optics by manufacturing arrays designed for specific purposes. Advances in micro- and nano-fabrication allow such micro-structured optical arrays to be made, one way being deep silicon etching using the Bosch process, which uses repetitive etch and passivate cycles, the latter to minimise sidewall etching. These offer the possibility of much better performances through greater flexibility in the choice of channel geometry. They can also have built-in adaptivity to correct aberrations and to control the focal length by, for example, coating the supporting spokes with piezo material.

The Abbe sine condition requires two reflections from the same wall of each channel, implying thick channels. This would lead to manufacturing difficulties (very high aspect ratios) and make the optics hard to bend. A solution is to use two parts (figure 8), aligned using micro-machined locators. The components can then be flexed independently, and more bending flexibility could be obtained by using a series of independent bimorph strips.

A first design (see table) is for the X-ray microprobe at the Gray Cancer Institute (GCI), which uses a microfocus source with a Ti target ( $K_{\alpha}$  at 4.5 keV). For the prototype, a single strip, giving a line focus of a point source, is used.

A 2 mm diameter optic with circular channels, 10  $\mu\text{m}$  wide and 200  $\mu\text{m}$  long, has been ray traced using Zemax (figure 9). The efficiency of each reflection was taken into account. Although the overall efficiency is less than 1%, for zero roughness the gain in focused flux over the alternative (a 100  $\mu\text{m}$  diameter, 10% efficient zone plate) is about 2 orders of magnitude. This is reduced by a factor of about 3 for a channel wall roughness of 10 nm.

Source size	5 $\mu\text{m}$
Source to optic	16 cm
Separation of optic components	1 mm
Length of channels	200 $\mu\text{m}$
Width of channels	10 $\mu\text{m}$
Bending radius of 2nd component	10 cm
Focal distance	7.3 cm

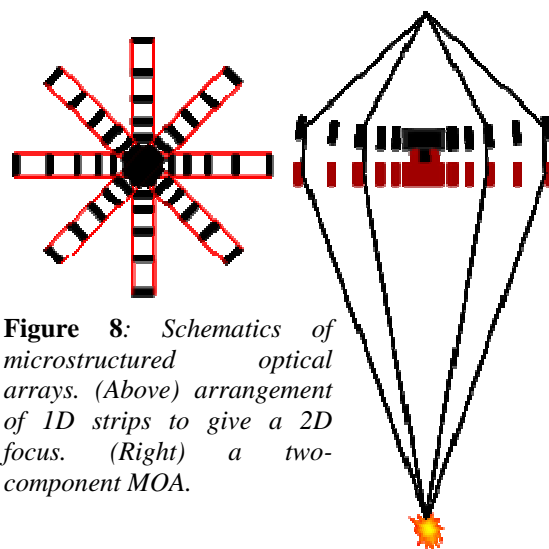


**Figure 8:** Schematics of microstructured optical arrays. (Above) arrangement of 1D strips to give a 2D focus. (Right) a two-component MOA.

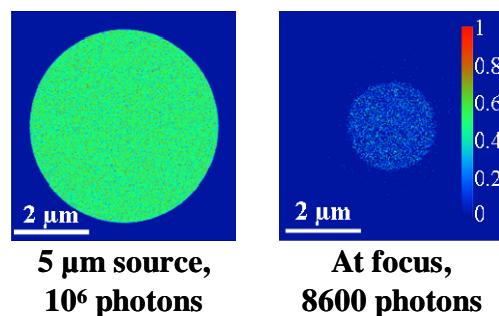


**Figure 9:** Zemax ray-tracing output.

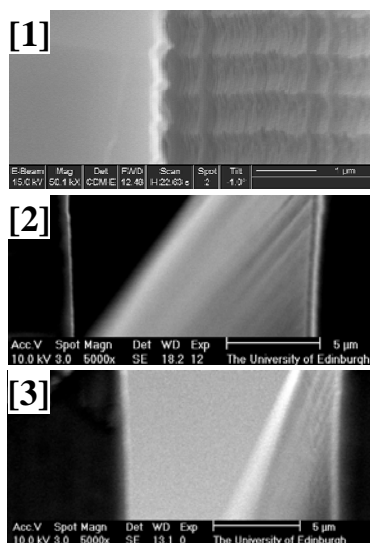


**Figure 10.** Improvement in sidewall characteristics. See text for details.



**Figure 11.** AFM lineouts before and after the oxidisation stage.

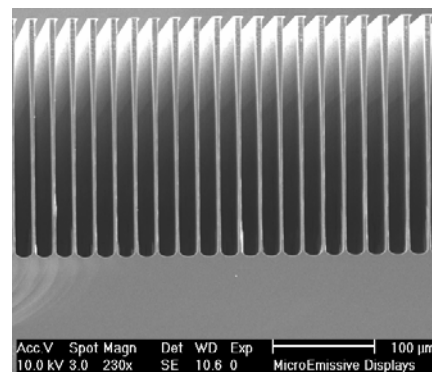


**Figure 12.** Smooth but curved sidewalls caused by simultaneous etch/passivate.

In the first attempt at making the prototype [1 in figure 10], both short scale roughness and figure errors were much greater than 10 nm. By shortening the Bosch process etch/passivate cycle the SMC team has significantly improved the channel wall quality [2]. Oxidising the surfaces (100 nm thick) and then removing the oxide layer by dipping in hydrofluoric acid, gives

further improvement [3]. AFM lineouts (figure 11) before oxidisation [4] show figure errors with periodicity  $\approx 30\ \mu\text{m}$  and amplitude  $\approx 50\ \text{nm}$ , with rms roughness  $\sigma \approx 18\ \text{nm}$ . Oxidisation and removal seems to eliminate the long range figure error, and reduce the rms roughness to  $\approx 8\ \text{nm}$  [5]. There may be a residual figure error with periodicity  $\approx 5\ \mu\text{m}$  and amplitude  $\approx 25\ \text{nm}$ ; if this is taken into account then  $\sigma \approx 5\ \text{nm}$ . Thus the roughness is at an acceptable level, although further improvement would be desirable. However, Zemax calculations show that the figure error needs to be improved, otherwise the optical quality will be impaired significantly.

It is believed that further substantial improvements are possible. The next steps will include:

- Higher aspect ratios (up to  $\sim 40:1$ ) leading to higher overall efficiencies
- Modelling and optimisation of new designs, including curved channels
- Further reduction of the etch/passivate cycle time
- Simultaneous etch/passivate; this can lead to curved channels, which may be advantageous
- The use of thicker ( $300\ \text{nm} - 1\ \mu\text{m}$ ) oxide layers
- Repetitive oxidisation/removal
- Metal coating of sidewalls

#### 4. Multilayer Supermirrors (KCL, GCI)

Multilayer components for a number of different energy ranges have been designed and measured. An example of the predicted (blue curve) and measured performances (green data points) of a multilayer Mo/Si designed for 20% reflectivity over a broad angular range ( $4-5^\circ$  grazing angle) at  $4.5\ \text{keV}$  is shown in figure 11. The measurements were carried out at GCI. The measured values are consistent with a rms roughness of  $0.4\ \text{nm}$  (red curve). Shortly (July 2005), further work will be done at the Bessy synchrotron in Berlin. These measurements will include three types of broadband multilayer components which have not previously been designed or measured:

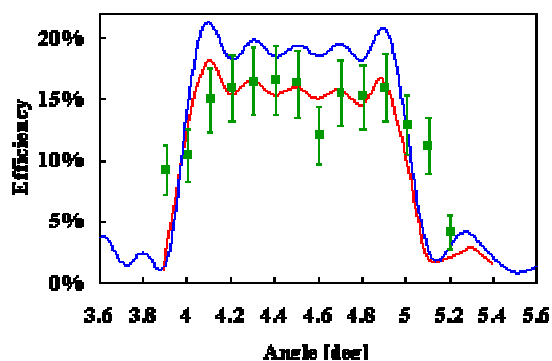


**Figure 11.** Calculated (blue curve) and measured (green data points) reflectivities of a broad angular range multilayer. The red curve is the calculated performance for an interlayer roughness of  $0.4\ \text{nm}$ .

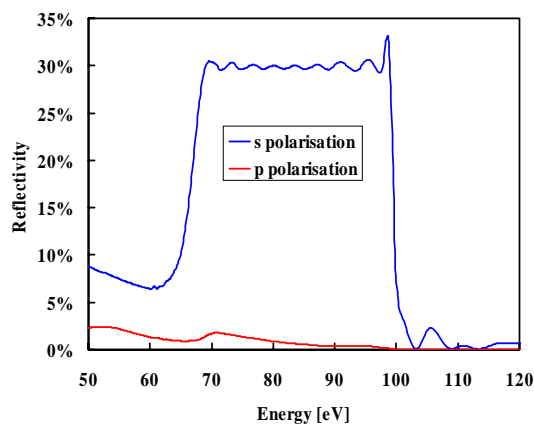


**Figure 12.** Calculated reflectivities of a broad spectral range multilayer polariser.

- Mo/Si wideband polarisers in the range  $69-99\ \text{eV}$ , covering the silicon and aluminium L edges. The reflectivities of the s- and p-components will be measured as functions of energy over the design range; the predicted performance of a multilayer designed for a reflectivity of 30% for the s-component at  $45^\circ$  incidence angle is shown in figure 12.
- Mo/Si wideband phase shifters in the range  $82-95\ \text{eV}$ , covering the aluminium L edge. The transmission of the s- and p-components and the phase shift between the two components will be measured as functions of energy over the design range.
- La/B<sub>4</sub>C analysers for the range  $137-193\ \text{eV}$ , covering the phosphorous and sulphur L edges, and Mo/Y analysers for the range  $103-155\ \text{eV}$ , covering the phosphorous L edge, will be measured as functions of energy over the design range.

#### 5 Applications (All institutions)

Two applications have been referred to in the preceding sections, namely X-ray astronomy and the microprobing of biological cells for radiation damage studies. In the former the improved optics will provide substantially enhanced angular resolutions, with obvious benefits, while in the latter they will allow higher throughputs so that rare effects such as mutations (rather than cell death, which is less important in terms of cancer) to be studied. Two other exemplar applications which have been considered are X-ray microscopy and X-ray (more specifically, EUV) lithography.

X-ray microscopy is increasingly being applied in a wide range of research, including:

- high spatial resolution and quantitative compositional mapping of multi-component polymeric materials, polymer nanocomposites and magnetic domains
- qualitative orientational characterisation of semi-crystalline thin films and other locally orientated polymeric materials
- molecular structures of conjugate polymer electrolytes and electroluminescent materials
- variable polarisation studies of liquid surfaces; orientation of molecules on substrates
- structural characterisation of foodstuffs – starch granule gelatinisation

- chemical state imaging of hyper-accumulator plants, micro-organisms, biofilms, fungi, worms etc.; biochemical pathways, bio-availability and bio-remediation of toxic metals and radionuclides
- characterising metals and organic macromolecules in sulphides, soils, sediments and solutions
- mechanisms of silicification of cyanobacteria; organic templates for silica nanotube formation
- chemical state imaging of airborne particulates/ aerosols
- bio-mineralisation – textural and morphological information related to atomic-scale structures
- chemical state mapping of meteorites (including organics), pre-solar and cosmic dust, Martian samples
- redox state mapping of transition elements in rocks and minerals
- imaging cellular structures/ molecular components in fossil plants (chemotaxonomy), coals, etc.
- determination of structural organisation of chromosomes, protein and DNA distribution in cells
- ultrastructures in micro-organisms in presence of water and nutrient solutions with element specific mapping of sub-cellular structures; imaging bacterial spores; tomography of frozen cells
- localisation of surface macromolecules on bacterial biofilms – cell-cell interactions
- calcification of tissue and oxidative changes in proteins in cells

However, to date these have all been carried out at synchrotron sources, and it is evident that if this continues to be the case X-ray microscopy will never become a routine analytical tool such as light, electron and scanning probe microscopies. The improved optics offered by this project will allow similar work to be carried out using laboratory sources, as the potential exists for focused intensities several orders of magnitude higher than with a zone plate microscope. There will be some compromises such as less wavelength tunability; the intention is not to replace synchrotrons but to widen access to modern instrumentation.

The project undertook a review of the use of X-rays for photolithography, concentrating on soft X-rays / EUV radiation with energies around 100 eV, the range now generally accepted as becoming the industry standard for future generation lithography. The associated advantages and disadvantages are well known, but are reviewed here for completeness. Places where the envisaged advances in optical performance would be beneficial are highlighted.

- In order to reduce X-ray absorption and scattering, the systems would have to be operated in a vacuum or in helium. This could lead to complexity and cost, but the problem would be reduced if more X-ray flux could be collected.
- Conventional X-ray sources and optics produce flux at the wafer surface that is typically less than that available at longer wavelengths by a factor of around  $10^3$ . Unless improved flux gathering capabilities can be provided, photoresists would have to be developed with sensitivity better than  $10 \text{ mJ/cm}^2$  in order to prevent unacceptably long exposure times.
- Synchrotron X-ray sources are more powerful but the size and cost factors are prohibitive. Additionally, because of the collimation of the beam such sources can only readily be used in proximity printing.
- If proximity printing methods were to be used, i.e., without optics, then due to the finite source size, a penumbra would occur which would affect the final resolution of the printed features.
- The final resolution of a proximity system is also be limited by the printing gap. In practice this would have to be controlled to better than  $\pm 0.5 \mu\text{m}$ .
- In an X-ray projection system using multilayer optics, several reflections are needed (mask, demagnifying optics) are needed, leading to low overall efficiencies even if single reflection efficiencies are as high as 70%.
- In such systems, extremely tight tolerances would be required for the surface accuracy of the multilayers, amounting to  $<1 \text{ nm}$  at  $13 \text{ nm}$  wavelength. Even if the optics could be manufactured to this accuracy, thermal and stress effects would not certainly degrade the performance. Adaptive optics could be used to compensate for this.
- Because the wavelength is short, diffraction effects can be largely ignored, which is good. Standing waves would also no longer be a problem area, unlike in conventional exposure systems.
- The large depth of field available gives good process latitude.
- There is the possibility of high throughput because large areas can be irradiated, so long as flux limitations can be overcome.
- There is practically no field size limitation.
- Most particulate defects which affect longer wavelength exposures tend to be transparent to X-rays.

Another aspect in which the proposed optics could provide an advantage is that it may not be necessary to change the optics when reduced minimum feature sizes are required.

## 6 Management and Networking

The management of the project worked extremely well. Day-long meetings were held every three months during the project, hosted by each partner in turn. At these meetings, which were also open to researchers in the consortium institutions, presentations were made to review the progress of each institution, synergies were identified and future research directions decided upon. Copies of the minutes of these meetings (excluding material confidential to the consortium) and the presentations made at them are available on request. The work was also disseminated more widely through seminars and, for example, presentations at the bi-annual meetings of the European Science Foundation Cost P7 Action “X-Ray and Neutron Optics”; copies are also available of these presentations.

New consortium members with relevant expertise were identified during the programme including the University of Birmingham (ceramic actuators), the University of Leicester (space X-ray optics) and CCLRC Daresbury Laboratory (optical testing). These are included in the proposed new Basic Technology Consortium.